Magnetization of two-dimensional square arrays of nanomagnets

Y. Takagaki and K. H. Ploog

Paul-Drude-Institut für Festkörperelektronik, Hausvogteiplatz 5-7, 10117 Berlin, Germany

The interplay between dipole-dipole interaction, magnetocrystalline anisotropy, and disorder on the magnetic hysteresis in two-dimensional square arrays of nanomagnets is studied by numerically solving the Landau-Lifshitz equation. The interaction-induced frustration gives rise to even-odd oscillations in the magnetic properties when the system size is varied. The oscillations persist to remarkably large arrays with fluctuating amplitudes, evidencing the significance of the boundary effects and the competition among a number of quasistable orders of the magnetic moments. The hysteresis is strongly affected by the magnetocrystalline anisotropy and disorder. While both of them broaden the hysteresis loop, the remanence in the disordered system bears a universal value: almost half of the saturation magnetization.

I. INTRODUCTION

The sizes of magnetic media to record a single bit have decreased drastically in recent years in order to increase the capacity of storage.[1] The magnetic characteristics of a unit cell as well as the interaction among the cells are fundamentally altered during the course of the size reduction.[2] In islands of, for instance, Fe,[3,4] Co,[5,6] or permalloy[7,8] having the thickness of several tens of nanometers and the diameter of ~ 1 μm, the magnetic texture of the ground state involves vortices. The flux-closure-type magnetic configuration is favored to minimize the stray fields, i.e., to reduce the magnetostatic energy. When the diameter of the disks is reduced, the disks undergo a transition, in which they are occupied by only a single magnetic domain. The transition takes place as the vortex energy becomes more costly than the magnetostatic energy.[9] Below the critical size for the single-domain formation, magnetic disks are regarded as nanomagnets even in the demagnetized state. In this regime, interparticle interaction is expected to dominate the processes of magnetization reversal when an external magnetic field is varied.[10,11]

In this paper, we examine the hysteresis in the magnetization of square arrays of nanomagnets. The arrangement of the magnetic moments in finite-size arrays is calculated by numerically solving the Landau-Lifshitz equation. We investigate how the ordering of the magnetic moments generated by dipole-dipole interaction is altered by the boundary effects, magnetocrystalline anisotropy, and disorder.

II. MODEL

In our simulations, we assume that identical nanomagnets are to be placed, in the absence of disorder, at the lattice sites of square arrays having a lattice constant a. We treat the individual nanomagnet as a magnetic moment **M**. The magnetic moments interact with each other through dipole-dipole interaction. Our numerical analysis examines the configuration of the magnetic moments in the presence of an external in-plane magnetic field **H**.[12,13] The response of the magnetic moments to the magnetic field is calculated by solving the Landau-Lifshitz equation

$$\frac{d\mathbf{M}}{dt} = \gamma \mathbf{M} \times \mathbf{H}_{\text{eff}} - \alpha \frac{\mathbf{M} \times (\mathbf{M} \times \mathbf{H}_{\text{eff}})}{M_s}, \quad (1)$$

where γ is the gyromagnetic ratio, α is the damping coefficient, and $M_s = |\mathbf{M}|$. The second term on the right-hand side of the equation phenomenologically introduces the relaxation of the magnetic moment, forcing **M** to be oriented in parallel with $\mathbf{H}_{\text{eff}}$ after energy dissipation. We note that the above equation conserves the magnitude of the magnetic moment.

The effective magnetic field $\mathbf{H}_{\text{eff}}$ acting on the magnetic moment consists of the applied external magnetic field, the dipole fields, and the uniaxial anisotropy field

$$\mathbf{H}_{\text{eff}}^i = \mathbf{H} - \mathbf{H}_{\text{dp}}^i + 2K \frac{\mathbf{M} \cdot \mathbf{u}}{M_s^2} \mathbf{u}, \quad (2)$$

where **u** is a unit vector in the direction of the magnetocrystalline anisotropy and K is the strength of the anisotropy. The dipole field acting on the ith nanomagnet that originates from the rest of the nanomagnets in the array is given by

$$\mathbf{H}_{\text{dp}}^i = \sum_{j \neq i} \left[\frac{\mathbf{M}_j}{r_{ij}^3} - 3 \frac{(\mathbf{M}_j \cdot \mathbf{r}_{ij}) \mathbf{r}_{ij}}{r_{ij}^5} \right]. \quad (3)$$

We do not take into account the shape anisotropy of the nanomagnets, i.e., the nanomagnets are assumed to be circularly shaped (with an infinitesimally small radius). The effects of the shape anisotropy are, at least qualitatively, equivalent to those of the magnetocrystalline anisotropy.

We have calculated the time evolution governed by Eq. (1) using the fourth-order Runge-Kutta method.[14] We typically use a fixed time step $\Delta t = 0.1/(\gamma M_s)$. The time step is appropriately reduced when a positional disorder is introduced as the dipole field gets significantly strong for the nanomagnets with a small separation. Iterations are continued until the changes in the orientation of the magnetic moments become negligibly small. Since we employ the fourth-order Runge-Kutta algorithm instead of the second-order one, the convergence can be achieved with the above time interval, which is much larger than $\Delta t = 0.005/(\gamma M_s)$ used in

Refs. 12 and 15. As a consequence, the maximum lattice size in the present work far exceeds that in the study by Kayali and Saslow.[15]

In evaluating the magnetization curves, $|H|$ is initially increased to a large value in order to almost fully magnetize the arrays. While H is subsequently varied around zero with a small step (typically $\Delta H = 0.01 M_s/a^3$), a steady state is derived for each value of H. Throughout this paper, **H** is aligned along the axis of the square arrays and α/γ is set to be 0.6. For the several (general) cases that we checked in details, the numerical results were unchanged when these parameters were moderately altered. That is, as our attention is focused on the static properties of the magnetization, the numerical results to be presented below are, except for unusual circumstances,[16] independent of the specific choice of the damping parameter.[17]

III. MAGNETIC ORDERING DUE TO DIPOLE-DIPOLE INTERACTION

A. Symmetric arrays

We first examine the magnetic properties when only dipole-dipole interaction is accounted for. Prakash and Henley[18] investigated the ground state and the linear response to an external magnetic field of an infinite array within the approximation of nearest-neighbor interaction. The ground state was found to be infinitely degenerate. The continuous degeneracy is reduced to a discrete symmetry by the external field as certain states are selected. In finite arrays, boundary effects additionally play a crucial role in the ordering of magnetic moments. We have calculated the magnetization for square lattices of linear dimension N when H is varied. We emphasize that the long-range dipole-dipole interaction is fully taken into account in our simulations. The inset of Fig. 1(a) displays a hysteresis of the magnetization M_H per lattice site in the direction of H, i.e., along the axis of the square array. Here, the array contains $N \times N$ nanomagnets with $N=57$. The magnetocrystalline anisotropy is assumed to be absent ($K=0$). The magnetization and the magnetic field are normalized in units of M_s and M_s/a^3, respectively. The magnetic moments are nearly aligned along the external field when $|H| > M_s/a^3$. At weak magnetic fields, M_H changes roughly linearly with H. Nevertheless, a hysteresis is present in the magnetization curve and M_H exhibits small abrupt jumps at a number of values of H.

Figures 1(a) and 1(b), respectively, show the variation of the remanence M_0 and the area A_h enclosed by the hysteresis loop when N is changed. The magnetic field is varied between $-2M_s/a^3$ and $2M_s/a^3$, for which the magnetic moments are better than 99.5% polarized at $|H|=2M_s/a^3$. We find oscillatory behavior of M_0 and A_h when N changes between even and odd numbers.[15] The oscillations originate from the internal frustration imposed by the array boundary. The boundary effects were studied by Stamps and Camley[12] for the case of $N=3$. With increasing the array size, the boundary effects would be less important. The polarization at $|H_0|=2M_s/a^3$, for instance, improves for large values of N. Nevertheless, the magnitude of the even-odd oscillations remains significantly large even when $N \sim 60$. In fact, the os-
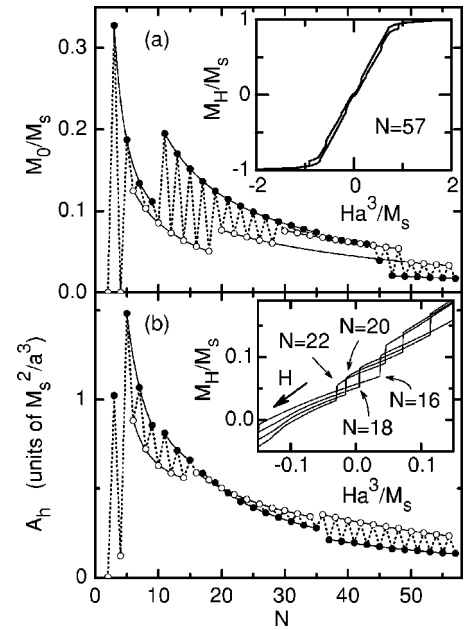

FIG. 1. (a) Remanence M_0 and (b) area A_h enclosed by the hysteresis loop when the size N of square arrays containing $N \times N$ nanomagnets is varied. The filled and open circles correspond to the odd and even values of N, respectively. The thin solid lines indicate the results of the fits using Eq. (4). The inset in (a) shows the magnetization M_H per lattice site when the external magnetic field H applied along the axis of the square array is varied for $N=57$. The magnetization curves for down magnetic-field sweep when $N=16$, 18, 20, and 22 are shown in the inset of (b). The uniaxial magnetocrystalline anisotropy is assumed to be absent ($K=0$).

cillation amplitude rather remains unchanged with N.

In the interior of square arrays, the magnetic moments are oriented, in the absence of an external field, along the rows or the columns of the arrays. The directions of the linearly aligned moments are antiparallel between adjacent lines.[12,18] Thus, M_0 is anticipated to be vanishingly small when the boundary effects are negligible. The microscopic configuration of the magnetic moments due to the internal frustration, which gives rise to the nonzero values of M_0, changes with N. However, certain magnetic textures are assumed to be intact for some intervals of N from the conservation of the oscillation amplitude. In Fig. 2, we show the magnetization pattern at $H=0$ when N is set to the specified values around 19. The magnetization pattern in the finite-size square arrays, in fact, exhibits domainlike structures. At the boundary between the "domain walls," one finds the "$\phi=\pi/4$" ground state[18] pointed out by Prakash and Henley, in which the nearest-neighbor magnetic moments are orthogonal to each other and the four magnetic moments in a unit cell of the square array form a closed loop. While N crosses the critical value between 18 and 20, where M_0 changes abruptly, the magnetization pattern does not change significantly. One noticeable change is that the zigzag of the magnetic moments at the right-end column is more pronounced for $N=20$ and 22 than that for $N=16$ and 18.

The difference in the magnetic texture is much greater between the even and odd numbers of N. Notice that both M_0 and A_h are larger for odd numbers of N than for even num-
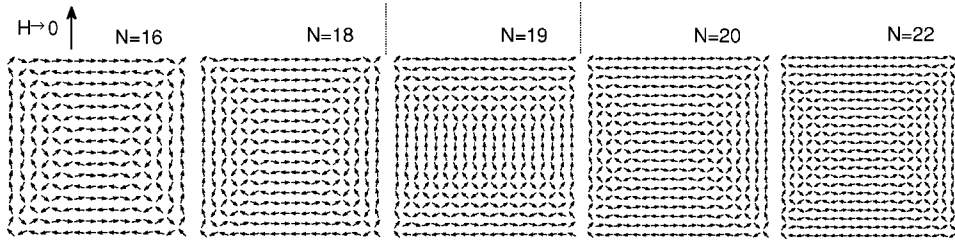
FIG. 2. Pattern of the magnetic moments at zero external magnetic field ($H=0$) for $N=16$, 18, 19, 20, and 22. The thick arrow indicates the direction of the external field.

bers when N is small, whereas the relationship is reversed when N is large. Therefore, the even and odd arrays are suggested to be governed by distinct order states of the magnetic moments. In Fig. 2, the antiparallel linear arrangement of the magnetic moments at the center of the arrays is perpendicular to the direction of the external magnetic field for the even numbers of N, whereas it is along the direction of the external field for $N=19$. (This feature is present also in the numerical results in Ref. 12 for the 5×5 and 6×6 arrays.) Interestingly, the magnetic moments of the outermost two columns are unusually parallel at the left- and right-hand sides for $N=19$, plausibly responsible for the larger M_0 than when N is even numbers.

The abrupt changes in the magnetic texture when N crosses critical values have a common origin with the abrupt jumps in M_H when H is varied. Notice that an abrupt change in M_0 does not necessarily result in the abrupt change in A_h, for instance between $N=18$ and 20. (A reverse situation can be easily caused by the emergence of an abrupt change of M_H at nonzero magnetic fields.) As shown in the inset of Fig. 1(b), the magnetic field for an abrupt change of M_H crosses $H=0$ between $N=18$ and 20 during the course of its gradual shift when N is varied.[19] (Another abrupt jump in M_H near $H=0.1M_s/a^3$ is responsible for the abrupt jump in M_0 between $N=28$ and 30.) A number of quasistable configurations evolve during the cycle of a magnetization curve. The even-odd oscillations in M_0 and A_h can thus be either in phase or out of phase.

The finite-size simulation by Stamps and Camley[12] was extended by Kayali and Saslow[15] up to $N=14$. From the behavior between $N=6$ and 14, A_h was suggested to be nonzero in the limit of $N \to \infty$. Similarly, a nonzero value of M_0 will be speculated for the infinite array if the same analysis is applied to the results in Fig. 1 in a similar range of N. As we stated, we anticipate, at least, M_0 to be zero in the absence of the boundary effects, as the antiferromagnetic-like columnar arrangement of the magnetic moments will prevail. Our much extended simulations demonstrate that the magnetic properties in the infinite system are hardly predictable by the extrapolation of the finite-size results because of the unsubsiding boundary effects. Given the domainlike structures demonstrated in Fig. 2, it seems rather unlikely that the boundary effects can be avoided by a mere extrapolation of $N \to \infty$. Nevertheless, following the analysis by Kayali and Saslow, we have attempted to fit the numerical data to the form

$$C(N) = C_\infty + \frac{C_{\mathrm{amp}}}{N^p}, \qquad (4)$$

where C is either M_0/M_s or $A_h/(M_s^2/a^3)$. As shown by the solid lines in Fig. 1, it is possible to fit the data with satis-

factory accuracies. It may be worthwhile to note that the values of M_0 for the two groups $N=20$, 22, 24, 26, and 28 and $N=50$, 52, 54, and 56 can be fit using common parameters. We summarize the fit parameters C_∞ and p in Fig. 3. The mean value of C_∞ is roughly zero for A_h, as expected. However, the mean value of C_∞ for M_0 appears to be unexpectedly negative.

The previous works by Stamps and Camley[12] and Kayali and Saslow[15] and the present work are based on the same numerical model. However, there are some differences among the numerical results. Kayali and Saslow found a "barrel" state at $H=0$ for $N=3$, in which the magnetic moments in the left and right columns are directed opposite to that in the central column and the corner moments are slightly tipped. The tipping was absent in the numerical result by Stamps and Camley. Consequently, the predicted magnetization loops are different between Refs. 12 and 15. We also find the barrel state, see the left inset of Fig. 7(b), in agreement with Kayali and Saslow. Nevertheless, our magnetization loop is somewhat different from their prediction, and A_h is larger in our case than theirs. In addition, our numerical result is considerably different from that of Kayali and Saslow when $N=5$. Our hysteresis loop, the dotted curve in Fig. 7(d), exhibits one less abrupt jump of M_H. Moreover, A_h in our simulations for $N=5$, 7, and 9 appears to form a group that is independent of the group consisting of $N=11$, 13, and 15. In contrast, Kayali and Saslow found that $N=7$,
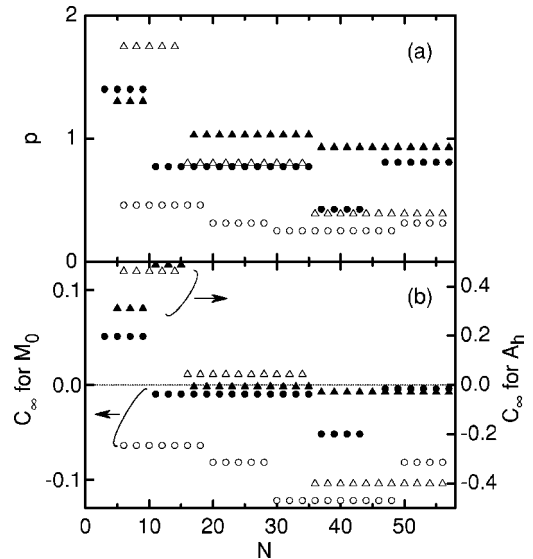

FIG. 3. Parameters p and C_∞, see Eq. (4), used in the fits shown by the solid curves in Fig. 1. The filled and open symbols correspond to the odd and even values of N, respectively. The circles and triangles indicate the values for M_0 and A_h, respectively.
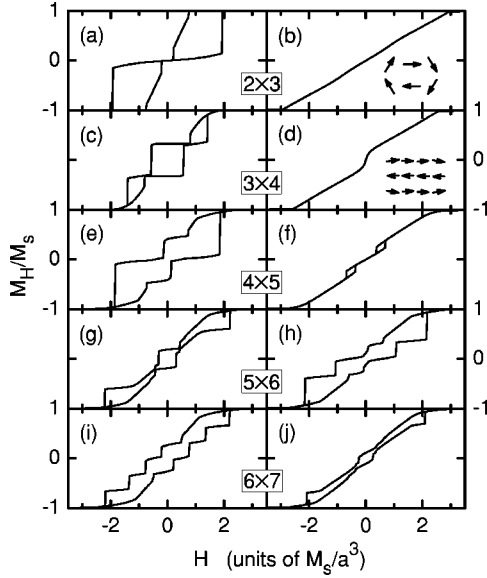
FIG. 4. Magnetization M_H per lattice site vs external magnetic field H of $N \times (N+1)$ asymmetric arrays in the absence of the uniaxial magnetocrystalline anisotropy. The number of the nanomagnets in the arrays is indicated in the panels. The magnetization is along the long and short directions of the arrays for the panels on the left- and right-hand sides, respectively. The configurations of the magnetic moments at $H=0$ for the 2×3 and 3×4 arrays are shown in the insets of (b) and (d), respectively.
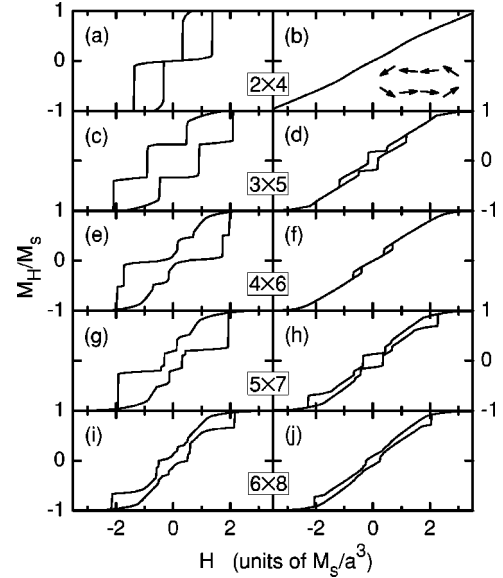
FIG. 5. Magnetization M_H per lattice site vs external magnetic field H of $N \times (N+2)$ asymmetric arrays in the absence of the uniaxial magnetocrystalline anisotropy. The number of the nanomagnets in the arrays is indicated in the panels. The magnetization is along the long and short directions of the arrays for the panels on the left- and right-hand sides, respectively. The configuration of the magnetic moments at $H=0$ for the 2×4 array is shown in the inset of (b).

9, 11, and 13 belong to the same group. Although these group assignments are not conclusive because of the short span of N for each group, our assignment is reasonable, at least for our results, since a large change is correspondingly present in M_0 between $N=9$ and 11.

B. Asymmetric arrays

The large even-odd oscillations suggest that the magnetic properties may exhibit a remarkable anisotropy when the number of the lattice sites is even in one direction and odd in the other direction. In Fig. 4, the magnetization curves are shown for asymmetric arrays consisting of $N \times (N+1)$ nanomagnets. The two horizontal panels are associated with an identical array: The magnetization is calculated along the long and short axes of the arrays for the left- and right-hand-side columns, respectively. We show the configurations of the magnetic moments at $H=0$ for the 2×3 and 3×4 arrays in the insets of Figs. 4(b) and 4(d), respectively. The configurations are independent of the direction of the external magnetic field. The hysteresis is absent in the short direction of the asymmetric arrays when the array size is small. (A comparison between the magnetization curves for the 2×3 and 3×4 arrays indicates that whether the number of nanomagnets in the magnetic field direction is even or odd is not relevant for the absence of the hysteresis.) This trend is, however, not a generic property of the asymmetric arrays as the hysteresis is more pronounced in the short direction for the array having 5×6 nanomagnets.

In asymmetric arrays, the magnetization is inevitably influenced by the shape anisotropy of the square lattices. In order to assess the contributions of the general, and hence less intriguing, shape anisotropy to the magnetization curves, we plot in Fig. 5 the hysteresis loops in arrays consisting of $N \times (N+2)$ nanomagnets. Despite the larger shape asymmetry for the $N \times (N+2)$ lattices than for the $N \times (N+1)$ lattices, the anisotropy in the magnetization curves in Fig. 5 is merely comparable to that in Fig. 4. We, therefore, conclude that the even-odd asymmetry gives rise to a considerable enhancement of the anisotropic magnetic properties.

IV. EFFECTS OF MAGNETOCRYSTALLINE ANISOTROPY

The importance of the internal frustration evidenced by the large even-odd oscillations suggests that the processes of the magnetization reversal are sensitive to perturbations that compete with the dipole-dipole interaction. In this and the next sections, we, respectively, examine the influences of the magnetocrystalline anisotropy and disorder, which cannot be ignored in the actual experiments.

The magnetocrystalline anisotropy is taken into account in Fig. 6 for the case of $N=24$. The easy axis of the uniaxial anisotropy is assumed to be 45° inclined from the axes of the square array within its two-dimensional plane. The magnetization flip processes are almost completely dominated by the magnetocrystalline anisotropy for $K \gtrsim M_s^2/a^3$. In such a circumstance, the magnetization curve of an array is, in principle, equivalent to that of a single nanomagnet. The magnetic moments are oriented in the diagonal direction of the array by the strong uniaxial anisotropy at $H=0$. The remanence is hence smaller by a factor of $1/\sqrt{2}$ than the fully
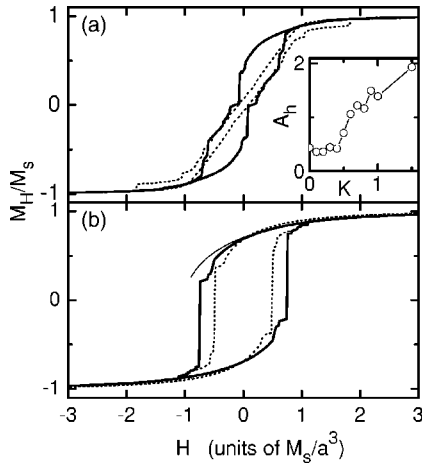
FIG. 6. Magnetization M_H per lattice site vs external magnetic field H as a function of the strength K of the uniaxial magnetocrystalline anisotropy. The easy axis of the uniaxial anisotropy is 45° inclined from the axes of the square array. For the dotted and thick solid curves, $Ka^3/M_s^2=0$ and 0.5 in (a) and 1.0 and 1.5 in (b), respectively. The linear dimension of the square array is $N=24$. The thin solid curve shows M_H when the dipole-dipole interaction is ignored, Eq. (5). The inset shows the area A_h of the hysteresis loop when the anisotropy strength K is varied. K and A_h are normalized both by M_s^2/a^3.

polarized magnetization. The external magnetic field rotates the magnetic moments to be away from the diagonal direction. The magnetization curve is, therefore, given by a gradual tilt of the magnetic moments determined by the balance between the external field and the anisotropy field. One finds from Eqs. (1) and (2)

$$H(\cos\theta-\sin\theta)=\frac{2\sqrt{2}K}{M_s}f(\theta)\sin\theta, \tag{5}$$

where θ is the angle of the magnetic moment with respect to the anisotropy axis and $f(\theta)=\cos\theta$ is the angular function of the magnetocrystalline anisotropy field. The thin solid curve in Fig. 6(b) is calculated using Eq. (5). Trivial cases are $\theta=0$ ($M_H=M_s/\sqrt{2}$) when $H=0$, and $\theta=\pi/4$ ($M_H=M_s$) when $H\to\infty$. When $|H|$ is increased with the opposite polarity, almost all the magnetic moments flip simultaneously at a critical magnetic field. The magnetization deviates from the prediction of Eq. (5) in the vicinity of this reorientation. The dipole-dipole interaction retains some influences on the reversal processes of the magnetization, owing to the subtle balance of the forces acting on the nanomagnets at the moment of the magnetization flip.

The magnetization curve when $K\sim0.5M_s^2/a^3$, the solid curve in Fig. 6(a), is a representative case in which the dipole-dipole interaction and the magnetocrystalline anisotropy compete with each other. The criticality of this value of K is illustrated by the expansion of the hysteresis loop due to the anisotropy, as displayed in the inset of Fig. 6. On the one hand, the dipole-dipole interaction prefers antiparallel repetition of collinear moments. On the other hand, the magnetocrystalline anisotropy orients all the magnetic moments in the direction favored by H and its previous history. The mag-
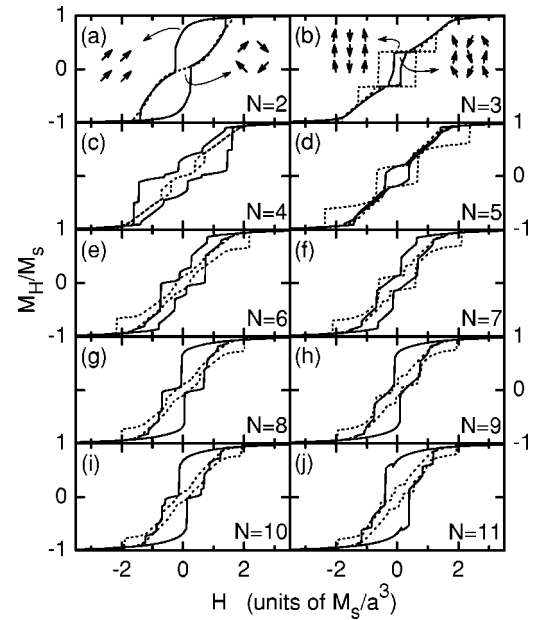

FIG. 7. Magnetization M_H per lattice site vs external magnetic field H in the simultaneous presence of dipole-dipole interaction and uniaxial magnetocrystalline anisotropy. The strength of the anisotropy is $K=0$ and M_s^2/a^3 for the dotted and solid curves, respectively. The easy axis of the uniaxial anisotropy is 45° inclined from the axes of the square array. The linear dimension N of the square arrays is indicated in each panel. The configurations of the magnetic moments at $H=0$ are shown for $N=2$ and 3 in the insets of (a) and (b), respectively.

netization curve for $K=0.5M_s^2/a^3$ is characterized by a convex-shaped gradual change of M_H, due to the force balance described by Eq. (5), while H is reduced to zero and a series of cascades, instead of a single giant jump, after the polarity of H has been reversed.

The competition between dipole-dipole interaction and magnetocrystalline anisotropy gives rise to dramatic effects in the hysteresis when the arrays are small, as the frustration is enhanced under the constraint of the boundary. In Fig. 7, we compare the magnetization curves in the presence and absence of the magnetrocrystalline anisotropy for various values of the size N of $N\times N$ square arrays. Here, $K=0$ and M_s^2/a^3 for the dotted and solid curves, respectively. For smaller arrays, larger values of K are required to heighten the competition as the ordering of the magnetic moments due to the dipole-dipole interaction is more stable. In fact, the magnetization curves for $K=0$ and $0.5M_s^2/a^3$ are almost identical when $N=2$. For this array size, the magnetic moments are made to be aligned along the anisotropy direction at $H=0$ by strengthening the anisotropy to $K=M_s^2/a^3$, see the inset of Fig. 7(a). The transition between the two stable states (around $H=0$) takes place abruptly at $K=0.774M_s^2/a^3$. When $N=3$, M_0 is similar for $K=0$ and M_s^2/a^3, see Fig. 7(b). However, the configuration of the magnetic moments at $H=0$ is considerably modified by the magnetocrystalline anisotropy.

In Figs. 6 and 7, the inclination of the magnetrocrystalline anisotropy from the axis of the array was assumed to be 45°. This angle was chosen primarily for correspondence to the existing experiments using Fe films epitaxially grown on
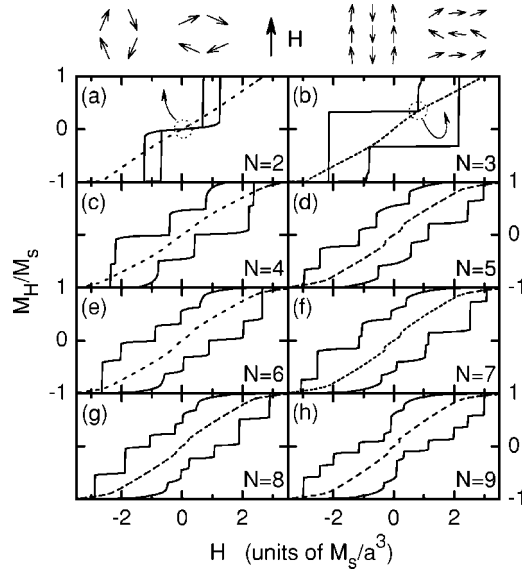
FIG. 8. Magnetization M_H per lattice site vs external magnetic field H in the simultaneous presence of dipole-dipole interaction and uniaxial magnetocrystalline anisotropy. The easy axis of the uniaxial anisotropy is parallel to one of the axes of the arrays. The strength of the anisotropy is $K=M_s^2/a^3$. The external magnetic field is along and perpendicular to the direction of the uniaxial anisotropy for the solid and dashed curves, respectively. The linear dimension N of the square arrays is indicated in each panel. The configurations of the magnetic moments at the indicated external magnetic fields are illustrated on top of the panels. The thick arrow indicates the direction of the external field. The easy axis of the uniaxial anisotropy is parallel and perpendicular to the external field for the configurations depicted on the left- and right-hand sides, respectively.

GaAs(001) substrates. As the dipole-dipole interaction is negligible in these experimental structures,[10] the arrays are usually defined, for convenience of sample fabrication, having their axes aligned along the cleavage direction of the substrate, i.e., {110}. The easy axes of the cubic anisotropy in the Fe films, which is dominant unless the films are considerably thin, are along the {100} direction of the substrate. (The cubic anisotropy was replaced by the uniaxial anisotropy in our simulations for simplicity.) For completeness, we have also carried out the simulations for the case of the uniaxial anisotropy being along one axis of the arrays. The magnetization curves when $K=M_s^2/a^3$ are presented in Fig. 8 for a number of array sizes. Because of the direct confrontation between the antiferromagnetic-like arrangement of the magnetic moments induced by the dipole-dipole interaction and the ferromagnetic-like arrangement favored by the magnetocrystalline anisotropy, the magnetization curves exhibit a dramatic dependence on the direction of the external magnetic field. Remarkably, hysteresis is absent in the magnetization curves for all the array sizes examined here when the external field is applied perpendicular to the direction of the uniaxial anisotropy.

V. EFFECTS OF POSITIONAL DISORDER

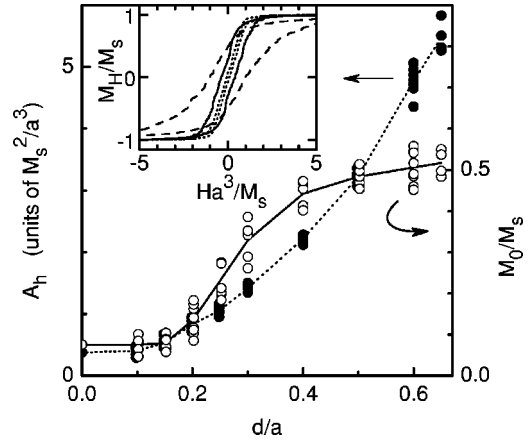We finally consider the influences of a disorder on the arrangement of magnetic moments governed by the dipole-

FIG. 9. Area A_h enclosed by the hysteresis loop (filled circles) and remanence M_0 (open circles) when the strength d of disorder is varied for the linear dimension of the square array $N=30$. The symbols indicate the values obtained for each realization of disorder. The lines show the statistically averaged values. The inset shows the magnetization M_H per lattice site vs external magnetic field H curves. The disorder strength is $d/a=0$, 0.3, and 0.6 for the dotted, solid, and dashed curves, respectively.

dipole interaction.[20,21] For this purpose, we displace the nanomagnets from the lattice sites of a square array. The amount of this displacement in the two orthogonal directions of the array is chosen randomly with a uniform distribution within an interval $[-d/2, d/2]$, i.e., the magnetic moment is placed completely randomly within a square area having the size $d \times d$ and centered at the lattice site of the nondisordered square array.

In the inset of Fig. 9, we compare the magnetization curves when $d/a=0.0$, 0.3, and 0.6 for $N=30$. One finds that the disorder enlarges the hysteresis loop in terms of both the remanence and the coercive field. The area A_h enclosed by the hysteresis loop and M_0 are plotted in Fig. 9. The symbols show the respective values for a certain realization of disorder. Statistically averaged ones are shown by the lines. The hysteresis in the disordered system has the following characteristics. (i) The enclosed area expands parabolically with increasing d. (ii) The remanence saturates at about one-half of the full magnetization when the disorder is strong. A large external magnetic field is required for fully polarizing the magnetic moments in the disordered system as the dipole field gets extremely strong for the nanomagnets with small separations. It may be noteworthy that, even though the disordered system lacks the spatial inversion symmetry, the magnetization curves for the up and down magnetic field sweeps are identical to each other if the polarities of H and M_H are simultaneously reversed, provided that $|H|$ reaches a large enough value.

VI. CONCLUSION

In conclusion, we have investigated the magnetization of square arrays of nanomagnets. The influences of dipole-dipole interaction on the processes of magnetic moment reversal have been examined through numerical solutions of

the Landau-Lifshitz equation. The internal frustration imposed by the array boundary persists up to considerably large arrays. A number of roughly degenerate magnetic configurations take over each other when the system size and the external magnetic field are varied. Kayali and Saslow[15] suggested that the area enclosed by a hysteresis loop in an infinite array is nonzero, based on the numerical results in finite-size arrays. Our much extended simulations indicate this prediction to be unreliable. The ordering of the magnetic

moments under dipole-dipole interaction has been demonstrated to be altered dramatically by the competition with the uniaxial magnetocrystalline anisotropy. We have also shown that a lattice disorder leads to an enlargement of the hysteresis loop if dipole-dipole interaction is significant. While the hysteresis loop expands its area parabolically with strengthening the disorder, the remanence is given universally to be about half of the saturation magnetization when the disorder is sufficiently strong.

[1] D. Weller and A. Moser, IEEE Trans. Magn. **35**, 4423 (1999).

[2] C. Kittel, Rev. Mod. Phys. **21**, 541 (1949).

[3] M. Hanson, C. Johansson, B. Nilsson, P. Isberg, and R. Wäppling, J. Appl. Phys. **85**, 2793 (1999); M. Hanson, O. Kazakova, P. Blomqvist, R. Wäppling, and B. Nilsson, Phys. Rev. B **66**, 144419 (2002).

[4] R. Pulwey, M. Zölfl, G. Bayreuther, and D. Weiss, J. Appl. Phys. **91**, 7995 (2002).

[5] M. Hehn, K. Ounadjela, J.-P. Bucher, F. Rousseaux, D. Decanini, B. Bartenlian, and C. Chappert, Science **272**, 1782 (1996).

[6] O. Kazakova, M. Hanson, P. Blomquist, and R. Wäppling, J. Appl. Phys. **90**, 2440 (2001).

[7] R. P. Cowburn, D. K. Koltsov, A. O. Adeyeye, M. E. Welland, and D. M. Tricker, Phys. Rev. Lett. **83**, 1042 (1999).

[8] M. Schneider, H. Hoffmann, and J. Zweck, Appl. Phys. Lett. **77**, 2909 (2000).

[9] P.-O. Jubert and R. Allenspach, Phys. Rev. B **70**, 144402 (2004).

[10] M. Grimsditch, Y. Jaccard, and I. K. Schuller, Phys. Rev. B **58**, 11 539 (1998).

[11] K. Y. Guslienko, Appl. Phys. Lett. **75**, 394 (1999).

[12] R. L. Stamps and R. E. Camley, Phys. Rev. B **60**, 11 694 (1999).

[13] G. Szabó and G. Kádár, Phys. Rev. B **58**, 5584 (1998).

[14] W. H. Press, B. P. Flannery, S. A. Teukolsky, and W. T. Vetterling, *Numerical Recipes in C: The Art of Scientific Computing*, 2nd ed. (Cambridge University Press, Cambridge, 1992).

[15] M. A. Kayali and W. M. Saslow, Phys. Rev. B **70**, 174404 (2004).

[16] C.-R. Chang and D. R. Fredkin, IEEE Trans. Magn. **22**, 391 (1986).

[17] The numerical iterations become large at magnetic fields where the magnetization abruptly changes and around zero magnetic field, implying that the configuration of the magnetic moments is considerably altered. The configuration may leap to a different quasistable state in these cases if the magnetic-field step or the damping parameter is too large.

[18] S. Prakash and C. L. Henley, Phys. Rev. B **42**, 6574 (1990).

[19] The exact value of the magnetic fields at which the magnetization discontinuously jumps depends somewhat on the choice of the magnetic-field step and the damping parameter (but not on the convergence criterion in our simulations). The critical sizes of the system for the abrupt jump in M_0, however, are not influenced by these parameters, unless the magnetic field for the discontinuous magnetization jump happens to be very close to zero.

[20] W. Luo, S. R. Nagel, T. F. Rosenbaum, and R. E. Rosensweig, Phys. Rev. Lett. **67**, 2721 (1991).

[21] P. J. Jensen and G. M. Pastor, New J. Phys. **5**, 68 (2003).